

# On the Optimal Braking of Wheeled Vehicles

PANAGIOTIS TSIOTRAS

*School of Aerospace Engineering*

*Georgia Institute of Technology, Atlanta, GA 30332-0150, USA*

CARLOS CANUDAS DE WIT

*Laboratoire d'Automatique de Grenoble*

*ENSIEG, BP 46, Saint-Martin-d'Herès Cedex, France*

## Abstract

The standard approach for designing ABS systems is to devise a control law to enforce operation at (or close to) the maximum of the friction force vs. slip curve. This “maximum friction” approach is based on the assumption that the friction force generated at the tire/ground interface can be accurately represented as a (static) function of the slip coefficient with a distinct maximum. Under this assumption, in this paper we provide a formal proof of this “maximum friction” approach using optimal control theory. The optimal control is shown to be singular and can be written in a state feedback form.

## 1 Introduction

It has been recognized for many years now that tire friction models play an important role in accurate prediction of vehicle behavior. The recent advances in anti-lock braking technology (ABS systems) make use of the knowledge of the friction force characteristics. One of the most popular strategies for minimum distance braking is operation at the maximum of the friction force. In this paper, we provide a formal proof of this “maximum friction” result by formulating the minimum braking distance problem as an optimal control problem which is subsequently solved using Pontryagin’s Maximum Principle. It is shown that, in the most general case, the optimal solution involves both subarcs of singular and bang-bang controls. In particular, it is shown that, under certain mild conditions, the singular control is the one that keeps the slip rate constant at the maximum friction value. In accordance with the classical results of optimal trajectories containing singular subarcs, the bang-bang controls are used to satisfy the initial and final boundary conditions.

A numerical example is used to calculate a typical optimal trajectory by solving the associated two-point boundary-value problem in terms of the state and co-state variables.

## 2 Tire Friction Models

We consider the longitudinal motion of a 1/4-vehicle wheel model, shown schematically in Fig. 1. The corresponding equations of motion can be derived directly from the figure as follows

$$m\dot{v} = F_r \quad (1a)$$

$$J\dot{\omega} = -rF_r + T, \quad (1b)$$

where  $m$  is 1/4 of the vehicle mass,  $r$  is the wheel radius,  $J$  is the moment of inertia of the wheel and drivetrain assembly,

$v$  is the velocity of the vehicle, and  $\omega$  is the angular velocity of the wheel.  $T$  is the braking torque (negative as shown), and  $F_r$  is the tire/road friction force (negative as shown).

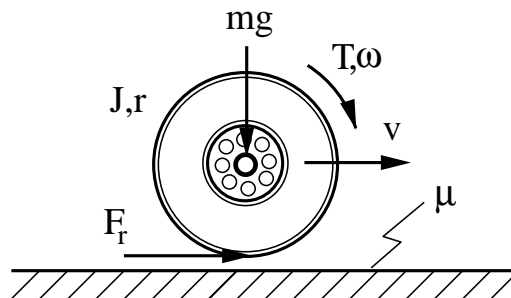


Figure 1: One-wheel schematic.

The friction force  $F_r$  depends on several factors (such as road conditions, tire characteristics, etc.) but it is primarily a function of the slip coefficient (or longitudinal slip rate)  $s$  defined by

$$s = \begin{cases} \frac{r\omega - v}{v} & \text{if } v > r\omega, \quad v \neq 0 \quad \text{braking/deceleration} \\ \frac{r\omega - v}{r\omega} & \text{if } v < r\omega, \quad \omega \neq 0 \quad \text{driving/acceleration} \end{cases} \quad (2)$$

Note that  $s < 0$  for braking and  $s > 0$  for driving under the previous definition of the slip. The friction force  $F_r$  has been notoriously difficult to model. Lumped [6], distributed [16, 15], static [14, 4] and dynamic models [6, 2, 7, 9] have been used in the past with various degrees of success.

One of the most widely used tire friction models is the one due to Pacejka (Pacejka’s “magic formula”) which gives the friction as a static map of the slip coefficient  $s$  as follows\*

$$F_r/F_n = D \sin(C \arctan(Bs)) \quad (3)$$

where  $F_n = mg$  is the normal force. The constants  $B, C, D$  are chosen to match the experimental data. A typical curve of friction vs. slip is shown in Fig. 2. It has a distinct local maximum at  $s^*$ . At that point maximum friction force occurs, i.e.,  $F_{\max} = F_r(s^*)$ .

\*This formula is the simplest version of the so-called “magic formula” and suffices to demonstrate the main ideas in this paper. More complicated expressions that capture very accurately experimental data not only of the longitudinal but also of the lateral and tire-aligning motions can be found, for instance, in [14, 1].

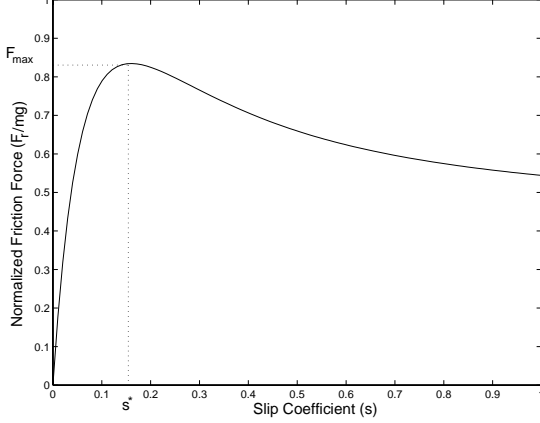


Figure 2: Friction force vs. slip coefficient.

The curve in Fig. 2 is derived under the assumption of steady-state conditions, i.e., constant  $v$  and  $\omega$ . Also, although Eq. (3) gives the friction force only as a function of the slip coefficient, in reality friction depends also on the vehicle speed, normal force, etc. In all cases however, the friction curve keeps its generic characteristics, having a unique maximum for some value of longitudinal slip. Based on this simple fact, several ABS system design are based on the reasonable conjecture that optimal (minimum traveled distance) braking occurs when the friction force operates at its maximum value (the “maximum friction” assumption). This conjecture is supported by the rationale that minimum traveled distance implies maximum deceleration, which in turn implies maximum friction force. Here we provide a formal proof of this result using optimal control theory. We also investigate the *exact* optimal, including the transition to and from the maximum friction condition.

### 3 Optimal Control Formulation

Given the equations (1) the objective is to minimize the performance index

$$\mathcal{J} = \int_0^{t_f} v(\tau) d\tau \quad (4)$$

subject to the following initial and final conditions

$$v(0) = v_0, \quad \omega(0) = \omega_0, \quad v(t_f) = \omega(t_f) = 0 \quad (5)$$

Using  $x_1 = v$  and  $x_2 = r\omega$  Eqs. (1) can then be re-written in the form

$$\dot{x}_1 = f(x) \quad (6a)$$

$$\dot{x}_2 = -\rho f(x) + u \quad (6b)$$

where

$$f(x) = \frac{F_r}{m}, \quad \rho = \frac{mr^2}{J}, \quad u = \frac{rT}{J} \quad (7)$$

Let  $x$  denote the state vector  $x = [x_1 \ x_2]^T$ .

The Hamiltonian associated with the previous optimal control problem is given by

$$\mathcal{H} = x_1 + \lambda_1 f(x) + \lambda_2 u - \lambda_2 \rho f(x) \quad (8)$$

The adjoint system is the given by

$$\dot{\lambda}_1 = -1 - (\lambda_1 - \lambda_2 \rho) \frac{\partial f}{\partial x_1} \quad (9a)$$

$$\dot{\lambda}_2 = -(\lambda_1 - \lambda_2 \rho) \frac{\partial f}{\partial x_2} \quad (9b)$$

Since the final time is not specified, the transversality condition gives

$$\mathcal{H}(t_f) = 0 \quad (10)$$

Along with the fact that the Hamiltonian is not an explicitly function of time, the last equation implies that

$$\mathcal{H}(t) = 0 \quad \forall t \in [0, t_f] \quad (11)$$

along the optimal trajectory.

The optimal control is given by

$$u_{\text{opt}} = \operatorname{argmin} \mathcal{H}(x, \lambda, u) \quad (12)$$

It is assumed that the control input  $u$  is bounded, that is, any allowable control must satisfy the constraint

$$u_{\min} \leq u \leq 0 \quad (13)$$

From (8) the switching function is

$$\mathcal{H}_1 = \lambda_2 \quad (14)$$

and using Eqs. (12)-(13), one obtains the following optimal control strategy

$$u_{\text{opt}} = \begin{cases} u_{\min} & \text{for } \mathcal{H}_1 > 0 \\ 0 & \text{for } \mathcal{H}_1 < 0 \\ u_{\text{sing}} & \text{for } \mathcal{H}_1 \equiv 0 \end{cases} \quad (15)$$

Note that the singular control  $u_{\text{sing}}$  is used when the switching function remains zero over a *finite* time interval, i.e.,  $\mathcal{H}_1(t) = 0$  for  $t \in [t_1, t_2] \subset [0, t_f]$ . Since in this interval the switching function is zero, taking the derivative of  $\mathcal{H}_1$  yields,

$$\dot{\mathcal{H}}_1 = \dot{\lambda}_2 = -(\lambda_1 - \rho \lambda_2) \frac{\partial f}{\partial x_2} \quad (16)$$

On the singular arc  $\lambda_2 \equiv 0$ , thus

$$\dot{\mathcal{H}}_1 = -\lambda_1 \frac{\partial f}{\partial x_2} \quad (17)$$

Setting the above expression to zero, differentiating once more, and setting the resulting expression to zero, one obtains

$$\ddot{\mathcal{H}}_1 = \frac{\partial f}{\partial x_2} + (\lambda_1 - \rho \lambda_2) \frac{\partial f}{\partial x_1} \frac{\partial f}{\partial x_2} - \lambda_1 \frac{d}{dt} \left( \frac{\partial f}{\partial x_2} \right) = 0 \quad (18)$$

or that

$$\ddot{\mathcal{H}}_1 = \frac{d}{dt} \left( \frac{\partial f}{\partial x_2} \right) = 0 \quad (19)$$

The calculation of the partial derivatives of the friction force gives

$$\begin{aligned} \frac{d}{dt} \left( \frac{\partial f}{\partial x_2} \right) &= \frac{\partial^2 f}{\partial x_2^2} \dot{x}_2 + \frac{\partial^2 f}{\partial x_1 \partial x_2} \dot{x}_1 \\ &= \frac{\partial^2 f}{\partial x_2^2} (-\rho f + u) + \frac{\partial^2 f}{\partial x_1 \partial x_2} f \end{aligned} \quad (20)$$

Equation (19) yields

$$\ddot{\mathcal{H}}_1 = \alpha(x) - \beta(x) u_{\text{sing}} = 0 \quad (21)$$

where

$$\alpha(x) = -\frac{\partial^2 f}{\partial x_1 \partial x_2} f + \rho \frac{\partial^2 f}{\partial x_2^2} f \quad (22a)$$

$$\beta(x) = \frac{\partial^2 f}{\partial x_2^2} \quad (22b)$$

Then, under the implicit assumption that  $\beta(x) \neq 0$ , the singular control is given by

$$u_{\text{sing}} = \frac{\alpha(x)}{\beta(x)} \quad (23)$$

For optimality, the control in Eq. (23) must also satisfy a local second-order convexity condition, known as the generalized Legendre-Clebsch condition or the Kelley-Contensou test [10]

$$\frac{\partial}{\partial u} \left( \frac{d^{2q} \mathcal{H}_1}{dt^{2q}} \right) \geq 0 \quad (24)$$

where  $q$  is the order of the singular arc. In our case,  $q = 1$  and (24) reduces to testing whether

$$\beta(x) \leq 0 \quad (25)$$

along the singular part of the trajectory.

#### 4 Computation of Singular Control

The computation of the singular control from Eq. (23) requires the calculation of the partial derivatives in (22). To proceed with the calculation of the singular control, we need to consider the explicit expression of the friction force as a function of  $x_1$  and  $x_2$ . Given the assumption that  $f$  is a function of only the slip coefficient  $s$  one obtains for the partial derivatives in (22)

$$\frac{\partial f}{\partial x_1} = \frac{\partial f}{\partial s} \frac{\partial s}{\partial x_1}, \quad \frac{\partial f}{\partial x_2} = \frac{\partial f}{\partial s} \frac{\partial s}{\partial x_2} \quad (26)$$

and hence

$$\frac{\partial^2 f}{\partial x_1 \partial x_2} = \frac{\partial^2 f}{\partial s^2} \frac{\partial s}{\partial x_1} \frac{\partial s}{\partial x_2} + \frac{\partial f}{\partial s} \frac{\partial^2 s}{\partial x_1 \partial x_2} \quad (27a)$$

$$\frac{\partial^2 f}{\partial x_2^2} = \frac{\partial^2 f}{\partial s^2} \left( \frac{\partial s}{\partial x_2} \right)^2 + \frac{\partial f}{\partial s} \frac{\partial^2 s}{\partial x_2^2} \quad (27b)$$

**Proposition 4.1** *On a singular subarc, necessarily*

$$\frac{\partial f}{\partial s} = 0 \quad (28)$$

*Proof.* On the singular arc  $\dot{\mathcal{H}}_1 = 0$  and from (17) one obtains that either  $\lambda_1 = 0$  or  $\frac{\partial f}{\partial x_2} = 0$ . If  $\lambda_1 = 0$ , the adjoint vector is identically zero on the singular subarc. We arrive at a contradiction since the adjoint vector cannot vanish anywhere [12]. Therefore, necessarily  $\frac{\partial f}{\partial x_2} = 0$  on the singular subarc. Since  $\frac{\partial s}{\partial x_2} \neq 0$  from the definition of the slip coefficient the chain rule yields  $\frac{\partial f}{\partial s} = 0$  along the singular subarc. ■

**Remark 4.1** From the proof of the Proposition it follows immediately that on a singular subarc necessarily  $\lambda_1 \neq 0$ . Since  $\partial^2 f / \partial x_2^2 \neq 0$  it follows that  $\beta(x) \neq 0$  and the expression for the singular control on a singular arc from Eq. (23) is well-defined. In addition, an allowable singular control must

satisfy the constraint in Eq. (13). Nevertheless, whether a singular control is part of the optimal trajectory depends also heavily on the problem boundary conditions. Appearance of the singular control in the composite optimal trajectory is not ensured *a priori*, even in the case the local optimality of the control law is guaranteed by the satisfaction of Kelley's condition (24). For most automotive applications, however, the maximum braking torque is large enough, such that a singular subarc is always part of the optimal trajectory. □

Notice that the expression of the singular control

$$u_{\text{sing}} = \frac{-\frac{\partial s}{\partial x_1} f + \rho \frac{\partial s}{\partial x_2} f}{\frac{\partial s}{\partial x_2}} \quad (29)$$

is in a purely *feedback* form (independent of co-states). Using Proposition 4.1, the partial derivatives in Eq. (27) can be computed as

$$\frac{\partial^2 f}{\partial x_1 \partial x_2} = \frac{\partial^2 f}{\partial s^2} \frac{\partial s}{\partial x_1} \frac{\partial s}{\partial x_2}, \quad \frac{\partial^2 f}{\partial x_2^2} = \frac{\partial^2 f}{\partial s^2} \left( \frac{\partial s}{\partial x_2} \right)^2 \quad (30)$$

From the definition of the slip coefficient for the braking case,  $s = x_2/x_1 - 1$ , one obtains

$$\frac{\partial s}{\partial x_1} = -\frac{x_2}{x_1^2}, \quad \frac{\partial s}{\partial x_2} = \frac{1}{x_1} \quad (31)$$

Equation (29) then yields

$$u_{\text{sing}} = \frac{x_2 f(x_1, x_2) + x_1 \rho f(x_1, x_2)}{x_1} \quad (32)$$

This is the expression of the singular control during braking. The only assumption used in the derivation of (32) is that the friction force is a function of the slip coefficient  $s$ . It should also be pointed out that the previous analysis does not hold for  $x_1 = 0$ . The classical treatment of friction using static maps breaks down at  $x_1 = 0$  (the slip coefficient is undefined at that point). This is the case when the wheel is spinning and the vehicle does not move. Although in a controlled braking case this cannot happen, this friction model does not work for a vehicle under continuous transitions between acceleration and deceleration phases or in very slow friction conditions. This drawback of static friction models has been recognized in the literature and offers one of the main motivations for developing dynamic friction models which remain well-defined everywhere [2, 3, 7, 6].

#### 5 Maximum Friction Control

Assuming that the friction force is given as a one-to-one map of the slip coefficient  $s$ , the control that keeps the friction force to its maximum value of the  $f$  vs.  $s$  curve (see Fig. 2) can be calculated by imposing  $\dot{s} = 0$ , along with the conditions

$$\frac{\partial f}{\partial s} = 0, \quad \frac{\partial^2 f}{\partial s^2} < 0 \quad (33)$$

Using the definition for the slip coefficient, and assuming that  $x_1 \neq 0$ , one obtains

$$\dot{s} = \frac{x_1 \dot{x}_2 - x_2 \dot{x}_1}{x_1^2} \quad (34)$$

Thus,  $\dot{s} = 0$  if and only if

$$x_1 \dot{x}_2 - x_2 \dot{x}_1 = -x_2 f(x) - \rho x_1 f(x) + x_1 u = 0 \quad (35)$$

or that

$$u_{f_{\max}} = \frac{x_2 f(x_1, x_2) + x_1 \rho f(x_1, x_2)}{x_1} \quad (36)$$

which is the same as the expression for the singular control in Eq. (32), under the additional assumption that  $\partial f / \partial s = 0$ . Therefore, the singular control  $u_{\text{sing}}$  achieves  $\dot{s} = 0$  and  $\partial f / \partial s = 0$ , i.e., it forces operation at the maximum of the friction vs. slip curve.

From (27b) the second condition in Eq. (33) implies that

$$\frac{\partial^2 f}{\partial x_2^2} < 0 \quad (37)$$

which is exactly Kelley's condition for optimality of the singular control.

It is clear that the singular control is constant. It can also be re-written as

$$u_{\text{sing}} = s^* f_{\max} + (1 + \rho) f_{\max} \quad (38)$$

The last expression has the advantage that it does not require the calculation of the partial derivatives in Eq. (27). It needs only the maximum value of the friction force  $f_{\max}$ , and the corresponding value of the slip coefficient  $s^*$ .

## 6 Numerical Example

To illustrate the previous analysis we consider a numerical example of minimum braking of a vehicle with mass 1000 kg ( $m = 250$  kg). The wheel radius is  $r = 0.25$  m and the wheel and drivetrain moment of inertia is  $J = 1$  kg m<sup>2</sup>. These values correspond to a value of  $\rho = 15.625$ . The initial conditions are given by  $x_1(0) = x_2(0) = 15$  m/s. To avoid the singularity of the friction model at  $x_1 = 0$  and  $s = 0$ , the final conditions are given by  $x_2(t_f) = 0.1$  m/s and  $x_4(t_f) = 0.099$  m/s. The initial conditions correspond to a value of the slip coefficient  $s(0) = 0$  and the final conditions correspond to a value of slip  $s(t_f) = -0.01$ .

The maximum value of the braking torque is given by  $T_{\max} = 1,500$  Nm which corresponds to  $u_{\min} = -375$ . For the Pacejka friction model the values  $D = 0.7$ ,  $B = 7$ ,  $C = 1.6$  where used. The maximum normalized friction force can be computed directly from Eq. (3) and is  $F_r/F_n = 0.7$ . The corresponding slip coefficient is  $s^* = -0.2138$ .

The state and co-state equations are numerically ill-conditioned. To numerically solve this two-boundary value optimization problem a special FORTRAN code was written based on a root-solving Newton method using the subroutine `hybrd` of the MINPACK library [13]. All calculations were performed using double precision arithmetic.

The results are shown in Figs. 3-4.

The optimal solution has three subarcs in this case. During most of the trajectory a singular control law is used to achieve maximum friction force. This is expected from the previous analysis. The initial and final bang subarcs take care of the required boundary conditions (slip not at the maximum friction force). The distance traveled before complete stop is  $\mathcal{J} = 16.382$  m. The total time to stop the vehicle under this applied braking torque profile (shown on the bottom of Fig. 4) is  $t_f = 2.17$  sec. The initial and final bang subarcs take place in a very short time interval. The duration of the initial and final subarcs are approximately 0.0123 and  $3 \times 10^{-4}$  seconds, respectively. That is, for all practical purposes, the initial and final bang subarcs can be

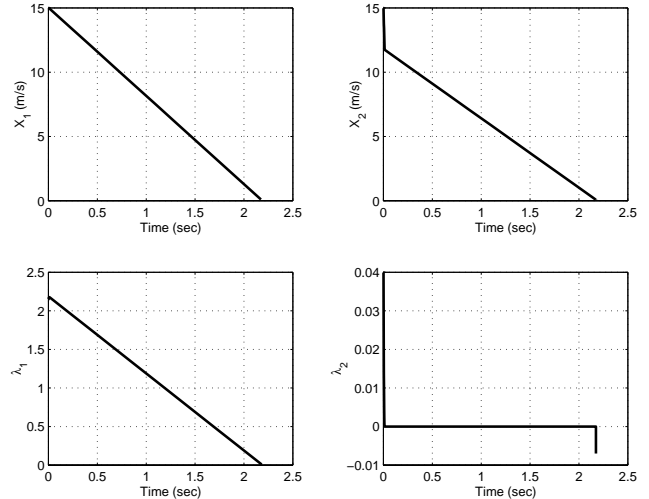


Figure 3: State and co-state time histories.

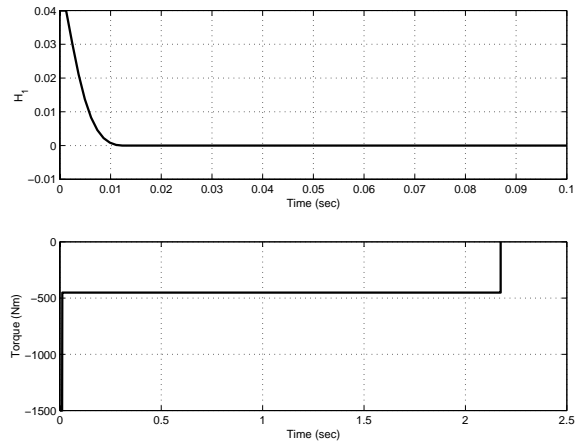


Figure 4: Switching function and braking torque history.

replaced by two impulses at the initial and final parts of the trajectory.

Figure 3 shows the time histories of the states and the co-states. The angular velocity of the wheel  $x_2$  and the corresponding co-state  $\lambda_2$  exhibit a very fast transient during the initial part of the trajectory, as expected from the optimal torque profile. The optimality of the trajectory is verified by the time history of the switching function  $\lambda_2$  in Fig. 3. A more detailed depiction of the switching function just before the entry to the singular subarc is shown on the top plot of Fig. 4. Finally, Fig. 5 shows the friction force and the slip coefficient history.

## 7 Conclusion

We have shown that the optimal braking strategy for a wheeled vehicle is to operate at the maximum point of the friction/slip curve. This strategy has been used extensively in the past in the design of ABS systems. One of the interesting results of our analysis is that the optimal "maximum friction" control is singular. Maximum torque control is used to match the boundary conditions. The total optimal trajectory is therefore composed of a sequence of bang-

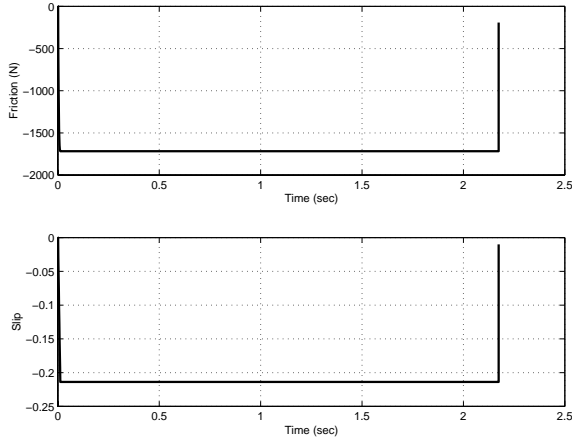


Figure 5: Friction force and slip coefficient time histories.

bang and singular arcs. For typical automotive applications, where the applied torque is high, the bang-bang subarcs can be safely approximated by impulses to achieve the specified boundary conditions of the slip.

The major drawbacks of the previous analysis are: First, it is based on the assumption that the friction force between the tire and the ground can be accurately described as a static relation in terms of the slip coefficient. In fact, it is well-known that transient effects can be important. This drawback can be addressed by incorporating recently developed dynamic friction models [6]. According to these results the friction force  $F_r$  is the output of a nonlinear filter which has as input the relative velocity  $v_r = x_2 - x_1$ . Specifically,

$$\dot{z} = v_r - \sigma_0 \frac{|v_r|}{g(v_r)} z \quad (39a)$$

$$F_r = (\sigma_0 z + \sigma_1 \dot{z} + \sigma_2 v_r) F_n \quad (39b)$$

where  $\sigma_0, \sigma_1$  are constants and  $z$  is the internal friction state. The function  $g(v_r)$  is given by

$$g(v_r) = \mu_c + (\mu_s - \mu_c) e^{-|v_r/v_s|^{1/2}} \quad (40)$$

where  $\mu_c, \mu_s$  and  $v_s$  are some constants. This tire friction model is based on the point LuGre friction model introduced in [5]. For more details on the tire friction model (39)-(40) refer to [6].

The static friction approach also requires prior knowledge of the maximum friction force and the corresponding optimal slip, which may not be readily known in a realistic environment of changing road and tire conditions. This drawback can be avoided, however, by implementing this optimal strategy via an “extremum seeking” control scheme, much in the same spirit as in Refs. [8] and [11].

## Acknowledgement

This work was performed during the visit of the first author at the Laboratoire d’Automatique de Grenoble during July 1999, as part of the CNRS/NSF collaboration project (NSF award no. INT-9726621/INT-9996096).

## References

- [1] E. Bakker, L. Nyborg, and H. Pacejka, “Tyre modelling for use in vehicle dynamic studies.” Detroit, MI, 1987. SAE Technical Paper 870421.
- [2] J. Bernard and C. L. Clover, “Tire Modeling for Low-Speed and High-Speed Calculations,” in *International Congress and Exposition*, (Detroit, MI), 1995. SAE Paper 950311.
- [3] P. Bliman and M. Sorine, “Easy-to-Use Realistic Dry Friction Models for Automatic Control,” in *3rd European Control Conference*, pp. 3788–3794, 1995. Rome, Italy.
- [4] M. Burckhardt, *Fahrwerktechnik: Radschlupfregelsysteme*, Berlin, Germany: Vogel-Verlag, 1993.
- [5] C. Canudas de Wit, H. Olsson, K. Åström, and P. Lischinsky, “A New Model for Control of Systems with Friction,” *IEEE Transactions on Automatic Control*, Vol. 40, No. 3, pp. 419–425, 1995.
- [6] C. Canudas de Wit and P. Tsiotras, “Dynamic Tire Friction Models for Vehicle Traction Control,” in *38th IEEE Conference on Decision and Control*, pp. 3746–3751, 1999. Phoenix, AZ.
- [7] C. L. Clover and J. E. Bernard, “Longitudinal Tire Dynamics,” *Vehicle System Dynamics*, Vol. 29, pp. 231–259, 1998.
- [8] S. Drakunov, Ü. Özgüner, P. Dix, and B. Ashrafi, “ABS Control Using Optimum Search via Sliding Modes,” *IEEE Transactions on Control Systems Technology*, Vol. 3, No. 1, pp. 79–85, 1995.
- [9] G. J. Heydinger, *Improved Simulation and Validation of Road Vehicle Handling Dynamics*, Ph.D. dissertation, Ohio State University, Columbus, OH, 1990. Department of Mechanical Engineering.
- [10] H. Kelley, R. Kopp, and H. Moyer, “Singular extremals,” in *Topics in Optimization*, New York: Academic Press, 1967.
- [11] M. Krstić and H.-H. Wang, “Design and stability analysis of extremum seeking feedback for general nonlinear systems,” in *Proc. of the 36th IEEE Conference on Decision and Control*, pp. 1743–1748, 1997. San Diego, CA.
- [12] E. B. Lee and L. Markus, *Foundations of Optimal Control Theory*, Malabar, Florida: R. Krieger Pub., 1986.
- [13] J. J. Moré, B. Garbow, and K. E. Hillstrom, “User Guide for MINPACK-1,” Technical Report ANL-80-74, Argonne National Laboratory, Applied Mathematics Division, Argonne, IL, 1980.
- [14] H. B. Pacejka and E. Bakker, “The Magic Formula Tyre Model,” in *Colloquium on Tire Models for Vehicle Dynamics Analysis*, Oct. 21-22 1991. Delft, The Netherlands.
- [15] A. van Zanten, R. Erhart, and A. Lutz, “Measurement and simulation of transients in longitudinal and lateral tire forces.” Detroit, MI, 1990. SAE Technical Paper 900210.
- [16] A. van Zanten, W. D. Ruf, and A. Lutz, “Measurement and Simulation of Transient Tire Forces,” in *International Congress and Exposition*, (Detroit, MI), 1989. SAE Technical Paper 890640.